C. R. Mecanique 338 (2010) 596–603

Contents lists available at ScienceDirect

Comptes Rendus Mecanique

www.sciencedirect.com

Micromechanics of granular materials

Micromechanical study of plasticity of granular materials ☆

Étude micromécanique de la plasticité des matériaux granulaires

Niels P. Kruyt

Department of Mechanical Engineering, University of Twente, NL-7500 AE Enschede, The Netherlands

ARTICLE INFO

Article history:
Available online 20 October 2010

Keywords:
Granular media
Plasticity
Micromechanics

Mots-clés :
Milieux granulaires
Plasticité
Micromécanique

ABSTRACT

Plastic deformation of granular materials is investigated from the micromechanical viewpoint, in which the assembly of particles and interparticle contacts is considered as a mechanical structure. This is done in three ways. Firstly, by investigating the degree of redundancy of the system by comparing the number of force degrees of freedom at contacts with the number of governing equilibrium equations; Secondly, by determining the spectrum of eigenvalues of the stiffness matrix for the structure that is represented by the particles and their contacts; Thirdly, by investigating the evolution with imposed strain of the continuum elastic stiffness tensor of the system. It is found that, with increasing imposed strain, the degree of redundancy rapidly evolves towards a state with small redundancy, i.e. the system becomes nearly statically determinate. The spectrum of the system shows many singular and near-singular modes at peak shear strength and at large strain. The continuum elastic stiffness tensor becomes strongly anisotropic with increasing imposed strain and shows strong non-affinity of deformation. The assumption of a constant and isotropic elastic stiffness tensor in elasto-plastic continuum constitutive relations for granular materials is generally incorrect. Overall, the plastic continuum behaviour of granular materials originates from the plastic frictional behaviour at contacts and from damage in the form of changes in the contact network.

RÉSUMÉ

La déformation plastique des matériaux granulaires est étudiée du point de vue micromécanique, dans lequel l'assemblage des particules et des contacts entre particules est considéré comme une structure mécanique. Ceci est fait de trois façons. Tout d'abord, en analysant le degré de redondance du système obtenu en comparant le nombre de degrés de liberté lié aux forces de contact avec le nombre d'équations d'équilibre; Deuxièmement, en déterminant le spectre des valeurs propres de la matrice de rigidité de la structure qui est représentée par les particules et leurs contacts; Troisièmement, en étudiant l'évolution pour une déformation imposée du tenseur de rigidité du milieu continu élastique équivalent au système analysé. Pour une déformation imposée, le degré de redondance évolue rapidement vers un état avec une petite redondance, c'est-à-dire que le système devient quasi isostatique. Le spectre des valeurs propres du système montre les modes singuliers et quasi singuliers au niveau de la résistance au cisaillement maximale et en grandes déformations. Le tenseur de rigidité élastique du milieu continu équivalent devient fortement anisotrope pour une déformation imposée, et fait apparaître la nature non affine de la

☆ This study is an extended version of that reported by N.P. Kruyt, L. Rothenburg, Plasticity of granular materials: a structural-mechanics view, in: M. Nakagawa, S. Luding (Eds.), Powders and Grains 2009, in: AIP Conference Proceedings, vol. 1145, 2009, pp. 1073–1076.

E-mail address: n.p.kruyt@utwente.nl.

1631-0721/$ – see front matter
doi:10.1016/j.crme.2010.09.005

déformation. L'hypothèse d'un tenseur de rigidité élastique, qui est constant dans des relations constitutives élasto-plastiques des matériaux granulaires, est généralement incorrecte. Globalement, le comportement macroscopique plastique est lié d'une part aux frottements aux contacts et d'autre part à l'évolution du réseau de contacts que l'on peut assimiler à un mécanisme d'endommagement.

1. Introduction

The mechanical behaviour of granular materials during quasi-static deformation is important in many disciplines of engineering, such as in civil, mechanical and process engineering, as well as in geophysics. This behaviour is described by the continuum-mechanical constitutive relation that links stress and strain increments. Often, elasto-plastic constitutive relations are employed that describe the yielding behaviour of granular materials.

At the micro-scale, granular materials consist of assemblies of particles that interact at contacts. In the micromechanical approach, which is complementary to the continuum-mechanical viewpoint, relationships are investigated between the micro-scale characteristics at the particle and interparticle level and macro-scale characteristics at the continuum level.

The objective of this study is to gain a better micromechanical understanding of continuum, macro-scale plasticity. This plastic behaviour is investigated from the structural–mechanical viewpoint, in which the granular assembly is considered as a mechanical structure that is determined by the particles and their interparticle contacts.

Three aspects are investigated from this structural–mechanical viewpoint: (1) the degree of redundancy of the system, by comparing the total number of force degrees of freedom at contacts with the number of equilibrium equations; (2) the spectrum of the structural–mechanical stiffness matrix of the discrete system; and (3) the evolution with imposed deformation of the elastic continuum stiffness tensor. These aspects are discussed consecutively, preceded by the relevant aspects of micromechanics of granular materials and of the two-dimensional Discrete Element simulations ([1], DEM for short) that are employed to obtain the required, detailed information at the micro-scale.

In the sign convention adopted here, compressive stresses and strains are considered as positive.

2. Micromechanics

Granular assemblies consist of particles that are generally very stiff. Therefore, the particles interact by point forces acting at interparticle *contacts*.

The position vector of a particle p is denoted by X_i^p. For two particles p and q in contact, the branch vector l_i^{pq} is the vector connecting the centres of two particles in contact, i.e. $l_i^{pq} = X_i^q - X_i^p$. In the two-dimensional case considered here, the normal and tangential vectors at the contact point are given by $n_i^{pq} = (\cos\theta^{pq}, \sin\theta^{pq})^T$ and $t_i^{pq} = (-\sin\theta^{pq}, \cos\theta^{pq})^T$, respectively, where θ^{pq} is the contact orientation.

The distribution of contact orientations in the contact network can be characterised by the contact distribution function [2] or by the second-order fabric tensor F_{ij} [3–5] that is defined by

$$F_{ij} = \frac{2}{N_p} \sum_{c \in C} n_i^c n_j^c \tag{1}$$

Here N_p is the number of particles in the assembly and the sum is over all contacts c in the set of contacts C. Coordination number Γ, i.e. the average number of contacts per particle, is defined by

$$\Gamma = \frac{2N_c}{N_p} \tag{2}$$

where the factor 2 is present since each contact is 'shared' between two particles (particle–wall contacts are ignored here). Hence, it follows from Eqs. (1) and (2) that $F_{11} + F_{22} = \Gamma$. As shown in [6], fabric anisotropy forms an important contribution to the shear strength of granular materials.

The contact constitutive relation, which relates force and relative displacement (increments) at the contact level, considered here is that described in detail in [1]. This contact constitutive relation involves elastic and Coulomb frictional effects. The elastic component of the constitutive relation is described by two linear springs in the normal and tangential direction at the contact with spring constants k_n and k_t, respectively. At a contact c, the elastic contact constitutive relation and the corresponding elastic contact stiffness matrix S_{ij}^c are given by

$$\mathrm{d}f_i^c = S_{ij}^c \, \mathrm{d}\Delta_j^c, \qquad S_{ij}^c = k_n n_i^c n_j^c + k_t t_i^c t_j^c \tag{3}$$

where $\mathrm{d}f_i^c$ is the force vector increment and $\mathrm{d}\Delta_i^c$ is the relative displacement vector increment at the contact point that involves contributions from the displacements of the particle centres as well as from the particle rotations.

For cohesionless granular materials, only compressive normal forces are possible. If the normal force were to become tensile, the contact is considered to be broken (or disrupted). The tangential force f_t^c at contact c is limited by Coulomb friction, i.e. $|f_t^c| \leqslant \mu f_n^c$ where f_n^c is the (compressive) normal force at the contact and μ is the interparticle friction coefficient.

The average stress tensor $\boldsymbol{\sigma}_{ij}$ can be determined from the contact forces f_i^c from (see, for example, [7]):

$$\boldsymbol{\sigma}_{ij} = \frac{1}{A} \sum_{c \in C} f_i^c l_j^c \tag{4}$$

where A is the area occupied by the assembly (including voids).

2.1. Structural–mechanical stiffness matrix

When the network of contacts is considered fixed, i.e. contact creation and contact disruption are ignored, and interparticle friction is neglected, then the assembly can be considered as a linear elastic mechanical structure. Its discrete structural–mechanical stiffness matrix can be determined from the geometry of the contacts and from the elastic contact stiffness matrices given by Eq. (3).

The equilibrium equations for force and moment for the particles in the assembly can be expressed formally as [8]:

$$\mathcal{K} \cdot \mathcal{U} = \mathcal{R}(\boldsymbol{\varepsilon}) \tag{5}$$

where $\mathcal{K}$ is the stiffness matrix of the system, $\mathcal{R}(\boldsymbol{\varepsilon})$ is the load which depends linearly on the imposed strain increment $\boldsymbol{\varepsilon}$, and $\mathcal{U}$ is the vector of displacement and rotation fluctuations of the particles, relative to the imposed mean-field. The size of the square matrix $\mathcal{K}$ is $3N_p$ by $3N_p$ and the length of the vectors $\mathcal{R}(\boldsymbol{\varepsilon})$ and $\mathcal{U}$ is $3N_p$. The method in which the (sparse, symmetric and non-negative) matrix $\mathcal{K}$ and the vector $\mathcal{R}(\boldsymbol{\varepsilon})$ are constructed is described in detail in [8].

When the vector with displacement and rotation fluctuations $\mathcal{U}$ has been computed from Eq. (5) for a prescribed loading path $\boldsymbol{\varepsilon}$, the total contact force at all contacts can be determined from the contact constitutive relation, Eq. (3), and the stress tensor from Eq. (4).

3. DEM simulations

Two-dimensional DEM simulations of biaxial deformation, in which the (principal) strain ε_{11} is imposed and the lateral (principal) stress σ_{22} is kept constant, have been performed. Two initial assemblies are considered, a 'dense' and a 'loose' assembly. Both assemblies consists of 50 000 polydisperse disks from the same lognormal particle-size distribution, for which the ratio of standard deviation over mean equals 0.25.

The two initial assemblies are isotropic, as characterised by the isotropy of the contact distribution function [2]. The packing fractions η, i.e. the area occupied by the particles divided by the total area occupied by the assembly, of the initial assemblies are $\eta = 0.844$ and $\eta = 0.814$ for the dense and the loose assembly, respectively. The corresponding coordination numbers are $\Gamma = 4.06$ and $\Gamma = 3.65$.

The isotropic confining stress in the initial state is denoted by σ_0. The parameters in the contact constitutive relation are selected such that $k_t/k_n = 0.5$ and $\sigma_0/k_n = 10^{-4}$. This latter quantity is non-dimensional in the two-dimensional case considered here. Its value is small, so the deformation at the contacts (or 'overlap' of the disks) is also small. Two values of the interparticle friction coefficient μ are considered, $\mu = 0.3$ and $\mu = 0.5$. Since two initial assemblies and two values for the friction coefficient are considered, the total number of DEM simulations equals four.

Periodic boundary conditions have been employed to minimize boundary effects and to suppress the formation of (global) shear bands in order to also investigate the behaviour at larger strains. No persistent, large-scale shear band was observed, although small-scale 'micro-bands' [9] are present.

The macroscopic response, in terms of shear strength $(\sigma_{11} - \sigma_{22})/(\sigma_{11} + \sigma_{22})$ and volumetric strain $\varepsilon_{11} + \varepsilon_{22}$ is shown in Fig. 1 (left) for the case of the dense initial assembly with friction coefficient $\mu = 0.3$. Note that with the adopted sign convention for strain, a positive value for $-(\varepsilon_{11} + \varepsilon_{22})$ corresponds to dilation. This response is typical for a dense initial assembly, showing some initial compression that is followed by dilation. The shear strength reaches its peak at a strain $\varepsilon_{11} \cong 1.7\%$, beyond which some softening occurs. Note that at an imposed strain $\varepsilon_{11} = 10\%$ the material still dilates, so a steady-state has not (yet) been attained.

The evolution with imposed strain ε_{11} of the fabric tensor F_{ij} is shown in Fig. 1 (right). It is clear that the number of contacts in the direction of applied strain shows a limited increase (the increase is about 10–20%), while that in the lateral direction rapidly decreases due to the macroscopic dilatancy that leads to the disruption of many contacts that are oriented in the direction of the minor principal stress σ_{22}. The component F_{11} of the fabric tensor is roughly independent of value of the friction coefficient μ, contrary to F_{22}. The loose initial assembly has a smaller anisotropy of the fabric tensor, expressed by $(F_{11} - F_{22})/(F_{11} + F_{22})$. A low coordination number or a low friction coefficient reduces the capability of the material to sustain large geometrical anisotropy. These results are similar to those reported in [6,10,11].

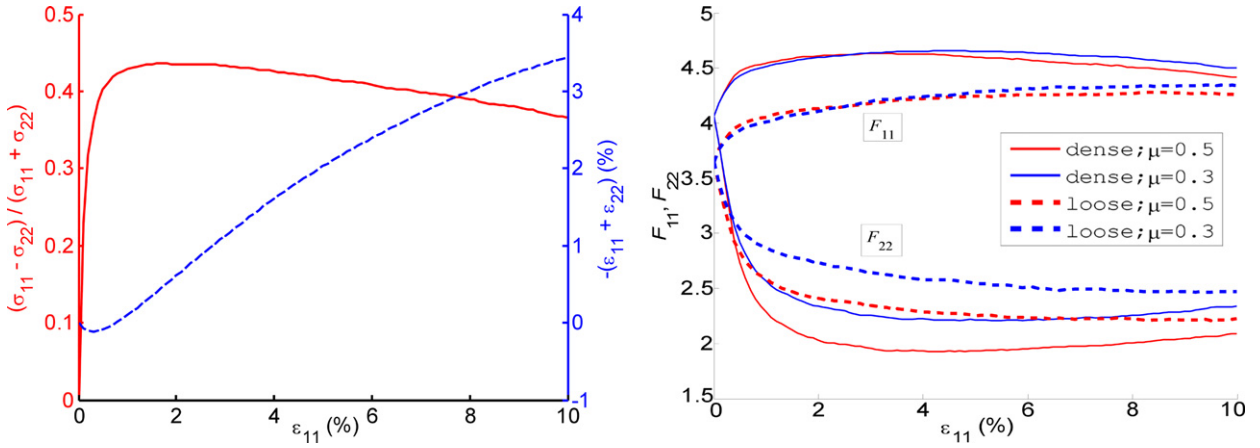

Fig. 1. Left: Evolution with imposed strain ε_{11} of the shear strength (solid line) and volumetric strain (dashed line); case of dense initial assembly with $\mu = 0.3$. Right: Evolution with imposed strain ε_{11} of the fabric tensor F_{ij}; $F_{12} = F_{21} = 0$.

4. Redundancy

The redundancy of the structure, represented by the assembly of particles and interparticle contacts, is investigated by comparing the total number of force degrees of freedom at contacts with the number of governing equilibrium equations for the particles, as was already suggested in [12].

The number of particles, excluding 'rattlers' (i.e. particles with zero contacts), is N_p. Such rattlers are excluded in the analysis, since they do not contribute to the force network, and hence to the stress. Note that a particle that is a rattler at a certain strain, can later during the deformation of the assembly come into contact with particles, and then it will no longer be considered as a rattler.

In the two-dimensional case considered here the number of force equilibrium equations is $2N_p$ and the number of moment equilibrium equations is N_p. Hence, the total number of equilibrium equations equals $3N_p$.

The number of contacts (excluding unstable contacts, i.e. contacts between particles that have only one or two contacts) is N_c. The number of contacts at which Coulomb friction is activated, i.e. where $|f_t^c| = \mu f_n^c$, is denoted by $N_{c,\mathrm{fr}}$. The number of elastic contacts at which Coulomb friction is not activated is $N_{c,\mathrm{el}}$. Note that

$$N_c = N_{c,\mathrm{fr}} + N_{c,\mathrm{el}} \tag{6}$$

The total number of force degrees of freedom at contacts is $2N_{c,\mathrm{el}} + N_{c,\mathrm{fr}}$, two forces for each elastic contact and one force for each contact at which friction is fully mobilised. The fraction of frictional contacts, S, is defined by

$$S = N_{c,\mathrm{fr}}/N_c \tag{7}$$

The evolution of S has been studied in [10] in various tests for (relatively small) three-dimensional assemblies consisting of (relatively soft) spheres. The influence of interparticle friction μ on the value of S at large strain in three-dimensional assemblies has been studied in [11].

The redundancy factor R is defined as the ratio of the total number of force degrees of freedom at contacts over the number of equilibrium equations

$$R = \frac{2N_{c,\mathrm{el}} + N_{c,\mathrm{fr}}}{3N_p} = \frac{2 - S}{6}\Gamma \tag{8}$$

where the latter equality follows from Eqs. (2), (6) and (7). This redundancy factor R must be larger than (or equal to) one for an equilibrium state to be possible. A value $R = 1$ corresponds to a statically-determinate (or isostatic) state. The isostaticity of assemblies of frictionless particles has been studied in [13–15], for example.

The evolution with imposed strain ε_{11} of the fraction of frictional contacts S is shown in Fig. 2 (left). The fraction of frictional contacts S quickly increases from a value of (almost) zero in the initial state and then remains constant. For the dense initial assembly a small reduction in the value of S is observed after the peak value is reached. The value of imposed strain at which the peak in S is reached is smaller than the value of strain at which the peak shear strength is attained, compare Fig. 1 (left) and Fig. 2 (left). The value at larger strains is the same for the dense and the loose initial assembly. As expected, for the lower value of the friction coefficient $\mu = 0.3$, the fraction of frictional contacts S is larger than for $\mu = 0.5$, since the Coulomb limit is attained more easily.

The evolution with imposed strain ε_{11} of the redundancy factor R is shown in Fig. 2 (right). The redundancy factor R quickly drops to a value close to one (or $R - 1$ drops to a value close to zero), the value at which the number of equilibrium equations equals the number of degrees of freedom at the contacts. In all four cases for large strains, the assembly is very

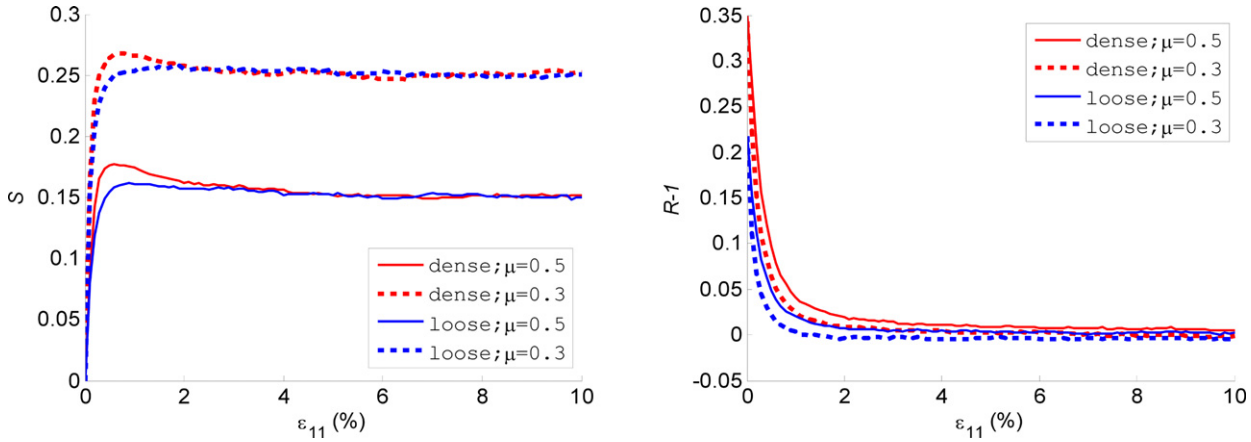

Fig. 2. Left: Evolution with imposed strain ε_{11} of the fraction of frictional contacts S. Right: Evolution with imposed strain ε_{11} of the redundancy factor R.

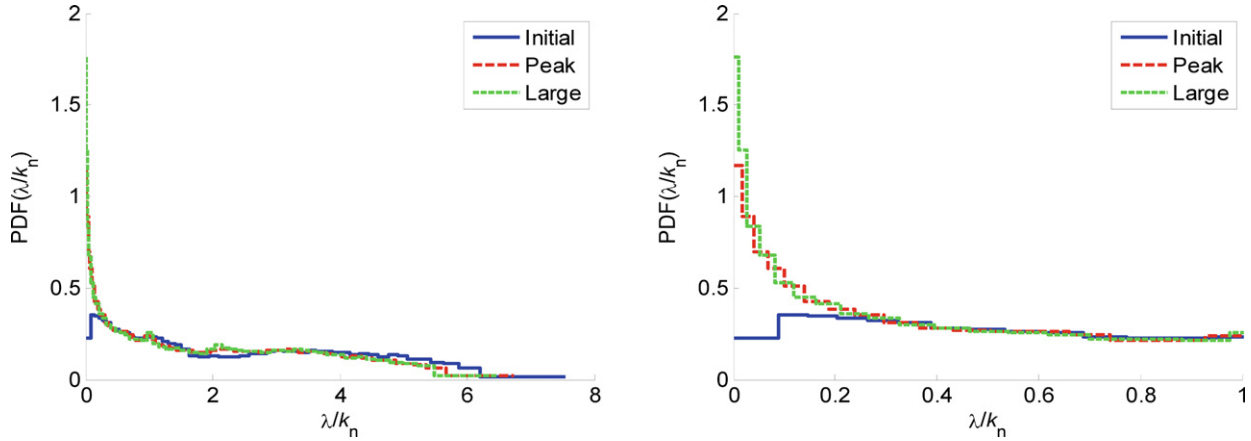

Fig. 3. Probability density functions for eigenvalues λ of the discrete stiffness matrix of the assembly, for the initial state, at peak strength and at large strain; case of a dense initial assembly and $\mu = 0.5$. Left: full range of eigenvalues; right: zoom-in on range of small eigenvalues.

close to a statically-determinate state, consistent with yielding or plastic behaviour, at the macro-scale continuum level. The reduction in the redundancy factor is faster for the lower value of interparticle friction coefficient μ. For the case with the loose initial assembly and the low value of interparticle friction coefficient $\mu = 0.3$, the redundancy factor drops very slightly below one (to a value of $R = 0.995$ on average). Although this is not possible for a strictly static system, it is noted that the deviation is small. This deviation may be due to the fact that the assembly moves dynamically through a sequence of nearly-static equilibrium configurations [16].

5. Spectrum of stiffness matrix

Here the spectrum, i.e. the set of eigenvalues $\{\lambda_e\}$, of the discrete structural–mechanical stiffness matrix of the structure (as outlined in Section 2.1) is investigated. The frictional state of (some of the) contacts is currently ignored.

Due to computer memory restrictions, it was not possible to compute the spectrum for the assembly of 50 000 particles. Therefore for a small system of 2000 particles, and hence 6000 degrees of freedom, that is similar to the large system of 50 000 disks studied here, the spectrum has been determined for the dense initial state, the state at peak shear strength and the state at large strain.

These three spectra are shown in Fig. 3 in the form of probability density functions for the eigenvalues (or 'densities-of-state'). Zero and near-zero eigenvalues have been removed (according to the criterion $\lambda/\lambda_{\max} < 10^{-10}$), as these correspond to rattlers and unstable configurations. The percentages of removed eigenvalues are 4% in the initial state, 11% at peak strength and 8% at large strain. A comparison of the spectra (based on the eigenvalues remaining after the removal of the zero and near-zero eigenvalues) in the initial state, at peak strength and at large strain shows that larger eigenvalues are present in the initial state (see Fig. 3, left) and that at peak strength and at large strain there is a large increase in the number of small eigenvalues (see Fig. 3, right). The large numbers of zero and near-zero eigenvalues correspond to deformation modes that are associated with small force changes. Hence, they are indicative of (localised) plastic deformation at

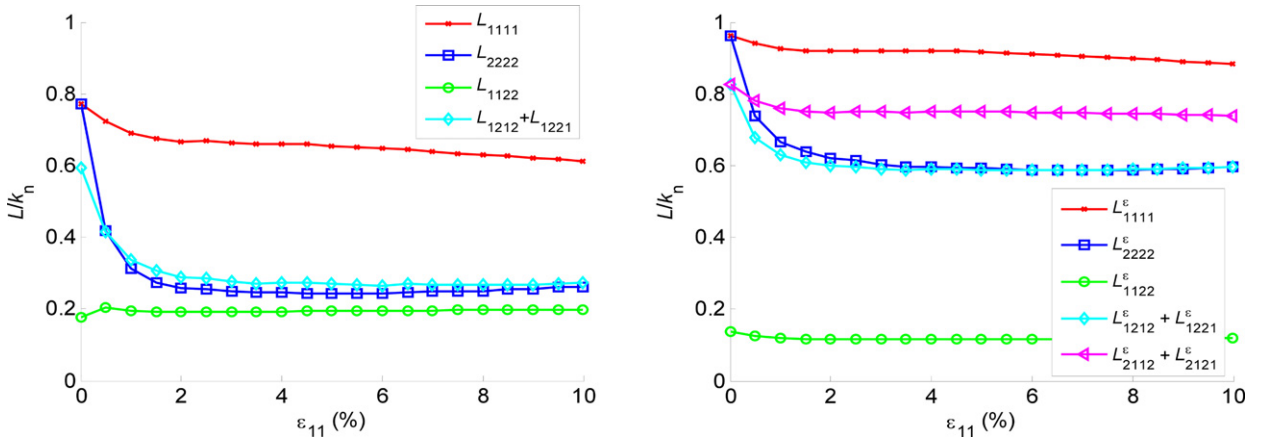

Fig. 4. Evolution with imposed strain ε_{11} of the actual stiffness tensor L_{ijkl} (left) and the uniform-strain stiffness tensor L^{ε}_{ijkl} (right). Case of dense initial assembly with $\mu = 0.3$. Since the strain tensor is symmetric, the combinations $L_{1212} + L_{1221}$ and $L_{2112} + L_{2121}$ are important for the shear stresses σ_{12} and σ_{21}, respectively.

the macro-scale continuum level. Note that for specifically constructed assemblies, non-local rolling deformation is possible [17]. For random, heterogeneous assemblies such non-local rolling deformation is unlikely to occur.

6. Elastic continuum stiffness tensor

By the definition of elastic deformation, the same stress path is followed upon reversal of the deformation. Upon reloading, the same response is obtained. However, DEM simulations of unloading and reloading from states along the biaxial deformation curve generally do not exhibit fully reversible behaviour, due to frictional forces and due to changes that occur in the contact network, arising from the continuous process of contact creation and disruption [18].

Therefore, elastic deformation is *defined* here as the deformation that occurs when the contact network is fixed and frictional constraints are ignored. Since the contact constitutive relation is linear, the macroscopic behaviour is linear and reversible, i.e. elastic. This elastic behaviour is completely determined by the imposed strain $\boldsymbol{\varepsilon}$ and the structural–mechanical stiffness matrix $\mathcal{K}$ (see Section 2.1).

Macro-scale, continuum elastic behaviour is characterised by the fourth-order elastic stiffness tensor L_{ijkl}. In the initial, geometrically isotropic state, this is an isotropic tensor that is described by the bulk and shear modulus (or equivalently, the Young's modulus and the Poisson's ratio).

In continuum plasticity theories, it is generally assumed that the elastic stiffness tensor L_{ijkl} is constant, i.e. it remains equal to the initial isotropic stiffness tensor. The results of the DEM simulations show that large changes occur in the fabric tensor F_{ij}: the contact geometry becomes strongly anisotropic with increasing imposed deformation ε_{11}, see Fig. 1 (right).

Therefore, the evolution of the elastic continuum stiffness tensor is investigated here in detail. In Section 2.1 it has been explained how the elastic stress response to an imposed strain increment can be computed from a DEM simulation with fixed and elastic contacts. By combining the information on the elastic stress response to a strain increment for three different loading paths (two uniaxial deformation paths in perpendicular directions and one simple shear deformation path), the full elastic stiffness tensor L_{ijkl} can be determined. The results for L_{ijkl} are shown in Fig. 4 (left) for the dense initial assembly with $\mu = 0.3$.

This stiffness tensor possesses the usual symmetries of stiffness tensors $L_{ijkl} = L_{jikl} = L_{klij}$. Components of the stiffness tensor that are not shown in Fig. 4 (left) are either zero (for example $L_{1112} = 0$) or reducible to those shown through these symmetry relations. The elasticity tensor is orthotropic with axes of symmetry that are defined by the principal axes of the fabric tensor [19]. Due to the changes in the fabric tensor, as shown in Fig. 1 (right), the elastic stiffness tensor becomes strongly anisotropic. In particular, the transverse stiffness L_{2222} rapidly decreases.

The micromechanical prediction of the stiffness tensor L_{ijkl} is much harder than may be expected, even in the isotropic state (see for example [8,16,20,21]). The simplest prediction is based on the uniform-strain assumption, according to which the relative displacement Δ^c_i at the contact is given by $\Delta^c_i = \varepsilon_{ij} l^c_j$ where l^c_i is the branch vector at the contact. The resulting elastic stiffness tensor L^{ε}_{ijkl} is given by [22–24]:

$$L^{\varepsilon}_{ijkl} = \frac{1}{A} \sum_{c \in C} S^c_{ik} l^c_j l^c_l \tag{9}$$

where A is the area occupied by the assembly. For *isotropic* assemblies it is well known that the actual deformation deviates from that according to the uniform-strain assumption [8,20,21,25,26]. This non-affinity results in deviations between the actual elastic moduli and those according to the uniform-strain assumption.

The evolution of L^{ε}_{ijkl} in the biaxial test, in which assemblies become (geometrically) anisotropic, is shown in Fig. 4 (right). By comparing the actual stiffness tensor and the uniform-strain stiffness tensor, the accuracy of the uniform-strain assumption of affine motion, can be evaluated for *anisotropic* assemblies. The large differences between L_{ijkl} and L^{ε}_{ijkl} that are apparent in Fig. 4 demonstrate the strong non-affine character of the motion, i.e. $\Delta^c_i \neq \varepsilon_{ij} l^c_j$.

From Fig. 4 (right) it follows that $L^{\varepsilon}_{1212} + L^{\varepsilon}_{1221} \neq L^{\varepsilon}_{2112} + L^{\varepsilon}_{2112}$ in anisotropic assemblies. In simple shear ($\varepsilon_{12} = \varepsilon_{21} \neq 0$, $\varepsilon_{11} = \varepsilon_{22} = 0$) it follows from Eq. (9) that according to the uniform-strain assumption

$$\sigma_{12} - \sigma_{21} = k_t\left(\bar{l^2}/A\right)\left(\sum_{c\in C}\left[\sin^4\theta^c - \cos^4\theta^c\right]\right)\varepsilon_{12}$$

where $\bar{l^2}$ is the average of the square of the (isotropically distributed) length of the branch vector and θ^c is the orientation of contact c. Hence, the uniform-strain assumption gives the prediction that for anisotropic assemblies $\sigma_{12} \neq \sigma_{21}$ in simple shear. This is incorrect, since the average stress tensor is symmetric (in the absence of contact couples) due to the moment equilibrium equations (see for example [27]). Note that the actual stiffness tensor always yields a symmetric stress tensor, thus L_{ijkl} satisfies $L_{1212} + L_{1221} = L_{2112} + L_{2112}$. The curve for $L_{2112} + L_{2112}$ is therefore not shown separately in Fig. 4 (left).

The changes in the elastic continuum stiffness tensor, that are caused by the changes in the fabric tensor, can be considered macroscopically as the result of a damage mechanism.

7. Conclusions

Continuum-mechanical plasticity of granular materials has been studied from the structural–mechanical viewpoint in three different ways:

1. By comparing the total number of force degrees of freedom at contacts with the number of equilibrium equations, i.e. by investigating the degree of redundancy of the system. This degree of redundancy depends on the coordination number and the fraction of frictional contacts.
2. By investigating the spectrum of eigenvalues of the discrete stiffness matrix for the structure that is represented by the particles and their interparticle contacts.
3. By investigating the evolution with imposed strain of the continuum elastic stiffness tensor of the system.

It is found that:

1. The degree of redundancy quickly evolves, with increasing imposed strain, towards a state with small redundancy, i.e. the system becomes (almost) statically determinate.
2. The spectrum of eigenvalues of the discrete stiffness matrix contains many singular and near-singular modes at peak strength and at large strain. Fewer large eigenvalues are present at peak strength and at large strain than in the initial state.
3. The continuum elastic stiffness tensor becomes strongly anisotropic with increasing imposed strain and it shows strong non-affinity of deformation.

All three ways of viewing the behaviour of granular materials from the structural–mechanical viewpoint show the signature of plastic behaviour at the continuum level. It is clear that employing a constant and isotropic elastic stiffness tensor in continuum elasto-plastic constitutive relations is generally not correct.

The plastic, irreversible behaviour at the continuum, macro-scale level involves of two mechanisms at the micro-scale level: Coulomb frictional behaviour at contacts and changes in the contact network, i.e. in fabric. The latter mechanism can be considered as a damage mechanism.

Acknowledgements

L. Rothenburg (University of Waterloo, Waterloo, Canada) and S. Luding (University of Twente, Enschede, the Netherlands) are thanked for valuable discussions.

References

[1] P.A. Cundall, O.D.L. Strack, A discrete numerical model for granular assemblies, Géotechnique 9 (1979) 47–65.
[2] M.R. Horne, The behaviour of an assembly of rotund, rigid, cohesionless particles I and II, Proceedings of the Royal Society of London A 286 (1965) 62–97.
[3] M. Oda, Initial fabric and their relation to mechanical properties of granular material, Soils and Foundations 12 (1972) 19–36.
[4] M. Satake, Constitution of mechanics of granular materials through graph theory, in: S.C. Cowin, M. Satake (Eds.), US–Japan Seminar on Continuum-Mechanical and Statistical Approaches to Granular Materials, Elsevier, Amsterdam, the Netherlands, 1978, pp. 47–62.
[5] K. Kanatani, Distribution of directional data and fabric tensors, International Journal of Engineering Science 22 (1984) 149–164.
[6] R.J. Bathurst, L. Rothenburg, Observations on stress–force–fabric relationships in idealized granular materials, Mechanics of Materials 9 (1990) 65–80.

[7] A. Drescher, G. de Josselin de Jong, Photoelastic verification of a mechanical model for the flow of a granular materials, Journal of the Mechanics and Physics of Solids 20 (1972) 337–351.
[8] N.P. Kruyt, I. Agnolin, S. Luding, L. Rothenburg, Micromechanical study of elastic moduli of loose granular materials, Journal of the Mechanics and Physics of Solids 58 (2010) 1286–1301.
[9] M.R. Kuhn, Structured deformation in granular materials, Mechanics of Materials 31 (1999) 407–429.
[10] C. Thornton, S.J. Antony, Quasi-static shear deformation of a soft particle system, Powder Technology 109 (2000) 179–191.
[11] A.S.J. Suiker, N.A. Fleck, Frictional collapse of granular assemblies, Journal of Applied Mechanics (Transactions of the ASME) 71 (2004) 350–358.
[12] P.A. Cundall, O.D.L. Strack, Modelling of microscopic mechanisms in granular material, in: J.T. Jenkins, M. Satake (Eds.), Mechanics of Granular Materials: New Models and Constitutive Relations, Elsevier, Amsterdam, the Netherlands, 1983, pp. 137–149.
[13] J.N. Roux, Geometric origin of mechanical properties of granular materials, Physical Review E 61 (2000) 6802–6836.
[14] J.N. Roux, G. Combe, Quasistatic rheology and the origins of strain, Comptes Rendus Physique 3 (2002) 131–140.
[15] C.S. O'Hern, L.E. Silbert, A.J. Liu, S.R. Nagel, Jamming at zero temperature and zero applied stress: the epitome of disorder, Physical Review E 68 (2003) 011306.
[16] N.P. Kruyt, L. Rothenburg, Shear strength, dilatancy, energy and dissipation in quasi-static deformation of granular materials, Journal of Statistical Mechanics: Theory and Experiment (2006) P07021.
[17] H.J. Herrmann, G. Mantica, D. Bessis, Space-filling bearings, Physical Review Letters 65 (1990) 3223–3226.
[18] L. Rothenburg, N.P. Kruyt, Critical state and evolution of coordination number in simulated granular materials, International Journal of Solids and Structures 41 (2004) 5763–5774.
[19] S. Nemat-Nasser, A micromechanically-based constitutive model for frictional deformation of granular materials, Journal of the Mechanics and Physics of Solids 48 (2000) 1541–1563.
[20] J.T. Jenkins, D. Johnson, L. La Ragione, H.A. Makse, Fluctuations and the effective moduli of an isotropic, random aggregate of identical, frictionless spheres, Journal of the Mechanics and Physics of Solids 53 (2005) 197–225.
[21] L. Rothenburg, N.P. Kruyt, Micromechanical definition of an entropy for quasi-static deformation of granular materials, Journal of the Mechanics and Physics of Solids 57 (2009) 634–655.
[22] R.J. Bathurst, L. Rothenburg, Micromechanical aspects of isotropic granular assemblies with linear contact interactions, Journal of Applied Mechanics (Transactions of the ASME) 55 (1988) 17–23.
[23] N.P. Kruyt, L. Rothenburg, Statistics of the elastic behaviour of granular materials, International Journal of Solids and Structures 38 (2001) 4879–4899.
[24] S. Luding, Micro–macro transition for anisotropic, frictional granular packings, International Journal of Solids and Structures 41 (2004) 5821–5836.
[25] H.A. Makse, N. Gland, D.L. Johnson, L.M. Schwartz, Why effective medium theory fails in granular materials, Physical Review Letters 83 (1999) 5070–5073.
[26] I. Agnolin, N.P. Kruyt, On the elastic moduli of two-dimensional assemblies of disks: relevance and modeling of fluctuations in particle displacements and rotations, Computers and Mathematics with Applications 55 (2008) 245–256.
[27] N.P. Kruyt, Statics and kinematics of discrete Cosserat-type granular materials, International Journal of Solids and Structures 40 (2003) 511–534.